Front. Earth Sci. 2013, 7(2): 141–150
DOI 10.1007/s11707-013-0355-1

RESEARCH ARTICLE

On summer stratification and tidal mixing in the Taiwan Strait

Jia ZHU, Jianyu HU, Zhiyu LIU (✉)

State Key Laboratory of Marine Environmental Science, College of Ocean & Earth Sciences, Xiamen University, Xiamen 361005, China

Abstract On continental shelves, a front that separates the sea into well-mixed and stratified zones is usually formed in warm seasons due to spatial variations of tidal mixing. In this paper, using eight years of in situ hydrographic observations, satellite images of sea surface temperature (SST) and chlorophyll-*a* (Chl-*a*) concentration, and results of a tidal model, we investigate summer stratification in the Taiwan Strait and its dependence on tidal mixing, upwelling, and river diluted water plumes. In most regions of the strait the dominant role of tidal mixing in determining the thermohaline structure is confirmed by the correlation between the two; there are some regions, however, where thermohaline structure varies in different ways owing to significant influences of upwelling and river diluted water plumes. The well-mixed regions are mainly distributed on the Taiwan Bank and in the offshore regions off the Dongshan Island, Nanao Island, and Pingtan Island, while the northern and central Taiwan Strait and the region south of the Taiwan Bank are stratified. The critical Simpson-Hunter parameter for the region is estimated to be 1.78.

Keywords Taiwan Strait, stratification, tidal mixing, coastal upwelling, river plume

1 Introduction

The important role of the turbulent mixing associated with tidal currents in setting up thermohaline structures on continental shelves has long been recognized (Dietrich, 1951). Based on simple energetic arguments, Simpson and Hunter (1974) proposed that the location of the frontal zone between tidally well-mixed and stratified regions can be well predicted by a critical value of the tidal mixing parameter (referred as the Simpson-Hunter parameter), h/u^3, where h is the water depth, and u is a velocity scale of the tidal currents, e.g., the amplitude of the predominant tidal constituent. The theory has successfully been used to locate tidal fronts on the continental shelves of the global ocean (Zhao, 1985; Garrett and Maas, 1993; Hu et al., 2003b; Lü et al., 2007; Holt and Umlauf, 2008).

The Taiwan Strait (TWS) is a waterway connecting the East China Sea (ECS) in the north and the South China Sea (SCS) in the south, and sandwiched by the China's mainland and Taiwan Island (Fig. 1). Most of the strait is shallower than 80 m with an average depth of about 60 m. The Taiwan Bank (TB) with depths of about 20–30 m, is located in the southern TWS. The Penghu Channel is located between the Penghu Archipelago and the Taiwan Island, descending southward sharply from 70 m to deeper than 1000 m. On the southern side of the strait, the SCS Warm Current flows northward through the Penghu Channel all year round (Chuang, 1986; Jan et al., 2002). In summer, the diluted waters originating from the Pearl River and the Hanjiang River intrude into the TWS, as evidenced by in situ observations (Li et al., 1998; Zhuang et al., 2003; Hong et al., 2009) and numerical simulations (Gan et al., 2009). In the offshore waters, the southwesterly wind in summer drives coastal upwelling, accompanied with strong fronts of sea surface temperature (SST) (Li et al., 2000; Hu et al., 2003a; Chang et al., 2006) and chlorophyll-*a* (Chl-*a*) concentration (Hu et al., 2001; Tang et al., 2002; Shang et al., 2004; Lan et al., 2009) between the upwelled water and the ambient waters. However, the situation becomes highly complicated as the three processes interplay with each other. For instance, the thermohaline structure in the TWS is not only greatly determined by the competition of solar heating and tidal mixing as in other tidally energetic shelf waters, but also significantly affected by the river diluted water plumes and upwelling. Understanding the interplay and the resulting thermohaline structure is of great importance to understanding regional physical and biogeochemical processes. Knowledge about this, however, has been very rare.

To this end, we attempt to shed light on the controling effects of tidal mixing, river plumes, and upwelling in setting up thermohaline structures in the TWS, based on

Received November 11, 2012; accepted December 14, 2012

E-mail: zyliu@xmu.edu.cn

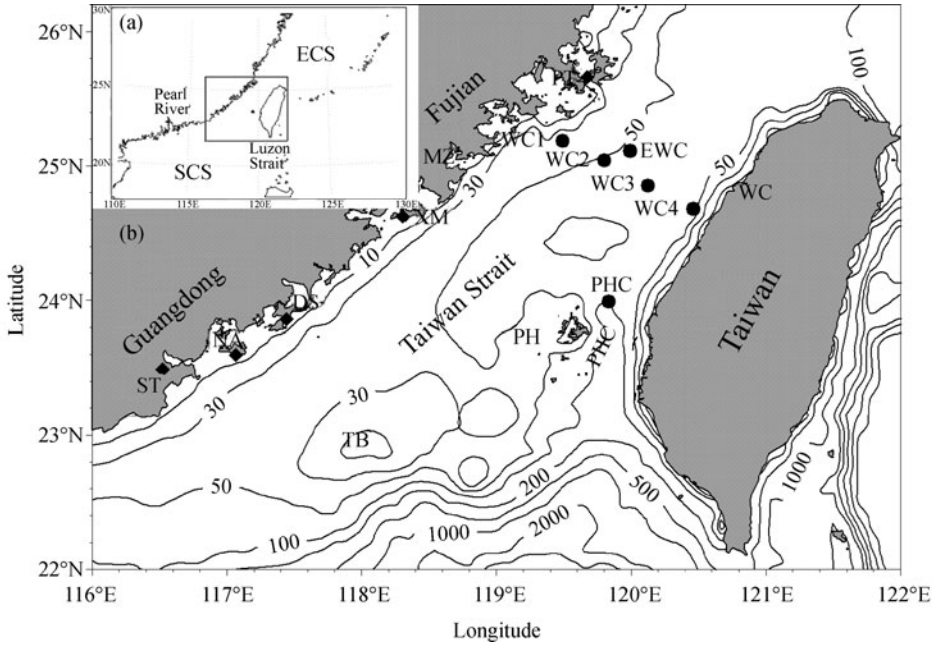

Fig. 1 Bathymetry of the study area. Acronyms: ECS-East China Sea, SCS-South China Sea, PT-Pingtan, MZ-Meizhou, XM-Xiamen, DS-Dongshan, NA-Nanao, ST-Shantou, WC-Wuci, TB-Taiwan Bank, PH-Penghu Archipelago, PHC-Penghu Channel. The depth contours are in meters. Inset shows the model domain.

eight years of in situ hydrographic observations, satellite images of SST, and Chl-*a* concentration, and tidal modeling results. We describe the horizontal distributions of vertical stratification in the TWS, and test the applicability of Simpson and Hunter's (1974) energetic arguments in locating the fronts. This paper is organized as follows: the observational data, analytical methodology, and details of the tidal model are introduced in Sect. 2. The results are analyzed in Sect. 3, in which the relationship between vertical stratification and intensity of tidal mixing is investigated, and the forming mechanisms of the SST and Chl-*a* fronts are discussed. Sections 4 and 5 give discussion and summary, respectively.

2 Data and analytical methodology

2.1 In situ observations

The Conductivity-Temperature-Depth (CTD) data used to analyze the thermohaline structures in the TWS were collected during Xiamen University's routine summer cruises during the eight years from 2004 to 2011. There were 452 station occupations, covering most regions of the TWS. Here we focus on analyzing the intensity and horizontal distribution of stratification.

The stratification of a water column can be characterized by several parameters, which are calculated from the observed temperature and salinity profiles. The buoyancy frequency profile, surface-bottom density difference, and the potential energy anomaly of the water column are the commonly used parameters. The standard deviations (STDs) of temperature and salinity profiles are also used to represent the intensity of stratification. In general, these two parameters are featured by the insensitivity to individual spikes and completeness of the CTD data. Thus, in this study we choose the STDs of temperature and salinity as the parameters characterizing the intensity of stratification, defined as:

$$\mathrm{STD}_1 = \left(\frac{1}{n}\sum_{i=1}^{n}\left(T_i - \overline{T}\right)^2\right)^{\frac{1}{2}}, \tag{1}$$

$$\mathrm{STD}_2 = \left(\frac{1}{n}\sum_{i=1}^{n}\left(S_i - \overline{S}\right)^2\right)^{\frac{1}{2}}, \tag{2}$$

where

$$\begin{aligned}\overline{T} &= \frac{1}{n}\sum_{i=1}^{n} T_i \\ \overline{S} &= \frac{1}{n}\sum_{i=1}^{n} S_i,\end{aligned} \tag{3}$$

where T_i and S_i are the temperature and salinity at the depth of z_i, and n is the number of samples in the profile. From the above definitions, one can see that the STD value is a direct measure of the temperature (salinity) difference in the profile, and thus usually the intensity of stratification. For weakly stratified water column, the STD values are very small, and close to zero when the water is well mixed

(i.e., the temperature and salinity are nearly constant in the water column). The larger the STD, the stronger the stratification, and vice versa. Besides the STDs, the original temperature and salinity profiles are also used to illustrate vertical thermohaline structure. Along one transect across the TB, the dissipation rates of turbulent kinetic energy ε were directly measured with an MSS-60 microstructure profiler (see Liu et al. (2009) for details of instrumentation and data processing) during the 2010 cruise. These provide ground-truth of turbulent mixing in the TWS. The tidal currents are predominant in the TWS; the turbulence is of mainly tidal origin and this is clearly reflected in the time-series measurements of ε (not shown in this paper).

2.2 Satellite images

In addition to in situ observational data, two Terra satellite Moderate Resolution Imaging Spectroradiometer (MODIS) images (SST on August 20, 2008 and Chl-*a* on July 9, 2009) are used to illustrate the spatial structures of SST and Chl-*a* concentration in the TWS. The spatial resolution of the images is 1 km.

2.3 Tidal current model

To simulate tidal currents in the TWS, a two-dimensional tidal current model including eight major tidal constituents (M_2, S_2, K_1, O_1, P_1, Q_1, N_2, and K_2) has been developed (Zhu et al., 2009). To minimize boundary effects, the computational domain is set to cover a large area of 110°E–130°E, 18°N–30°N, including the TWS, the southern ECS, the Pacific east of the Taiwan Island, and the Luzon Strait (Fig. 1). In the model, tidal currents are calculated by solving the primitive equations of the ocean. The equations are numerically solved with a second-order implicit difference method. The spatial resolution of the model is 6′ by 6′. The three open boundaries are forced with prescribed tidal elevations of the eight constituents; i.e.

$$\zeta_i = H_i \cos(\sigma_i t + v_{0i} - g_i), (i = 1,2,3,...,8), \quad (4)$$

where H_i is the amplitude of the i-th tidal constituent, g_i the phase, σ_i the angular frequency, and v_{0i} the astronomical initial phase. The harmonic constants of the tidal constituents at the open boundaries are extracted from a high resolution (0.5° by 0.5°) global model, the NAO-TIDE[1)].

The model results have been validated by the observations of tidal elevations and currents at eight stations (Jan et al., 2001; Qiu et al., 2002) in the TWS. As an example, the observed and modeled tidal current ellipses for the M_2 and K_1 tidal constituents are shown in Fig. 2. The mean relative biases of current direction for M_2, S_2, K_1, and O_1 tidal constituents are 9.0%, 2.7%, 11.3%, and 3.7%, respectively. In all, the two-dimensional model simulates tidal currents in the TWS well. This constitutes a basis for tidal mixing estimate in this study.

2.4 Tidal mixing parameter

Following Simpson and Hunter (1974), we calculate the tidal mixing parameter, i.e., the Simpson-Hunter parameter, from the modeled tidal currents,

$$K = \log_{10}(h/u^3), \quad (5)$$

where h is the mean water depth in meters, and u is the depth-averaged tidal velocity in $m \cdot s^{-1}$, including eight major tidal constituents. As interpreted by Simpson and Hunter (1974), the value of K reflects the mean intensity of tidal mixing through the water column at a specific location. As K decreases, either because the water depth h decreases or the tidal current u increases, tidal mixing becomes stronger. Therefore, for a typical coastal or shelf region without significant influence of river discharges and upwelling, quantity K is the main determinant of stratification.

3 Results

3.1 Distributions of stratification and tidal mixing

The spatial distributions of the temperature and salinity STDs are shown in Fig. 3. For further quantitative analysis, the study area has been divided into six sub-areas (termed as Areas A–F) based on the values of STDs. Examples of the vertical structure of the temperature and salinity from each area are shown in Fig. 4.

For the temperature, stations with the STD value below 2.0°C are shown with colors, and with gray levels for that above 2.0°C. For the salinity, stations with STD value below 1.0 are shown with colors, and with gray levels for that above 1.0.

As shown in Fig. 3(a), in the Area A, the STD of temperature is close to zero at most stations, extending from the Dongshan offshore area to the TB. This, together with the vertical structure of temperature as shown in Fig. 4, suggests that Area A is well mixed due to strong tidal mixing. Both Area B and Area C are weakly stratified with 0.78°C and 0.61°C of STD_1. The STD_1 is above 1.3°C in Areas D and F, implying strong stratification. In Area E, the mean STD_1 is above 4°C and the vertical temperature gradient is up to $0.12°C \cdot m^{-1}$ in the thermocline, implying a strong stratified area here, as well.

The STD of salinity (Fig. 3(b)) shows similar features to that of the temperature. The mean STD_2 in Area A is only

1) http://www.miz.nao.ac.jp/staffs/nao99/index_En.html

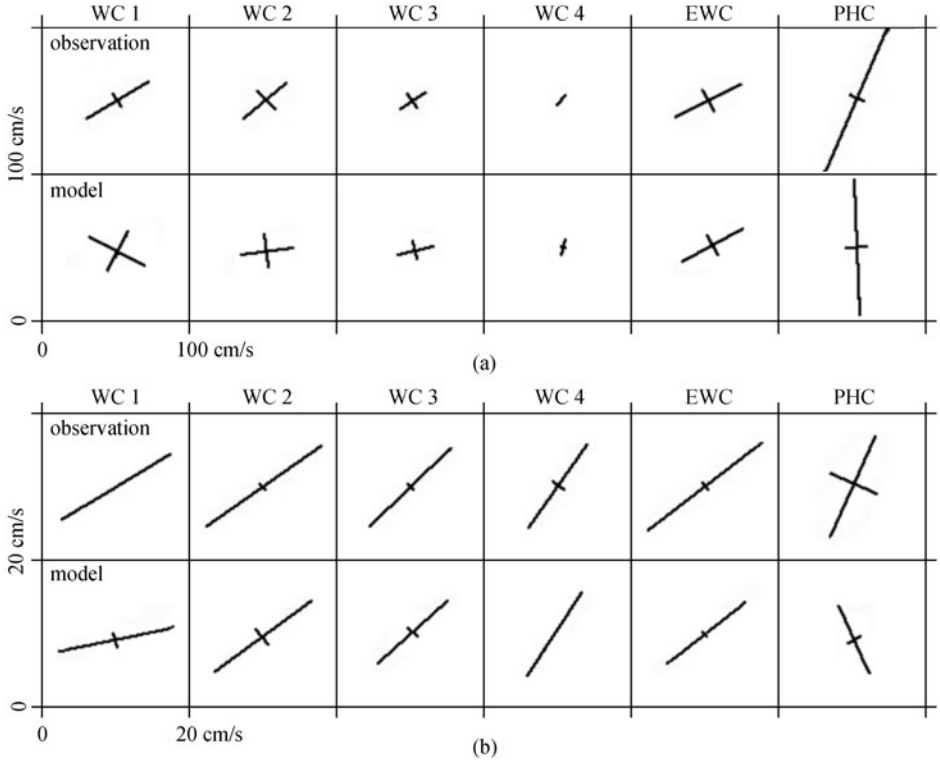

Fig. 2 Comparison between observed and modeled tidal current ellipse axes for the (a) M_2 and (b) K_1 tidal constituents at six stations in the TWS. The observations are adapted from Jan et al. (2001). The observational stations (WC1, WC2, WC3, WC4, EWC and PHC) are shown with black bullets in Fig. 1.

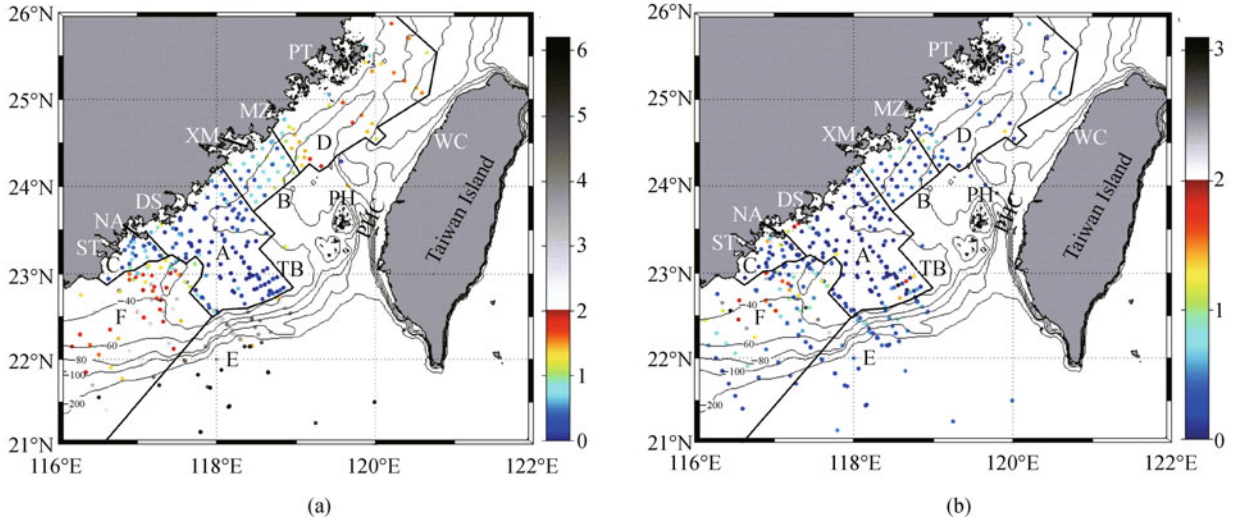

Fig. 3 Distributions of temperature (a) and salinity (b) STDs. The study area is divided into six regions: Areas A–F. Acronyms: PT-Pingtan, MZ-Meizhou, XM-Xiamen, DS-Dongshan, NA-Nanao, ST-Shantou, WC-Wuci, TB-Taiwan Bank, PH-Penghu Archipelago, PHC-Penghu Channel.

0.19, the smallest among all the areas. In Areas B and C, the mean STD_2 is 0.45 and 0.53, close to each other, but the maximum surface-bottom salinity difference is distinct, 0.85 for Area B and 3.28 for Area C. This is because the offshore region of Area C is under significant influence of the diluted water from the Hanjiang River. The mean STD_2

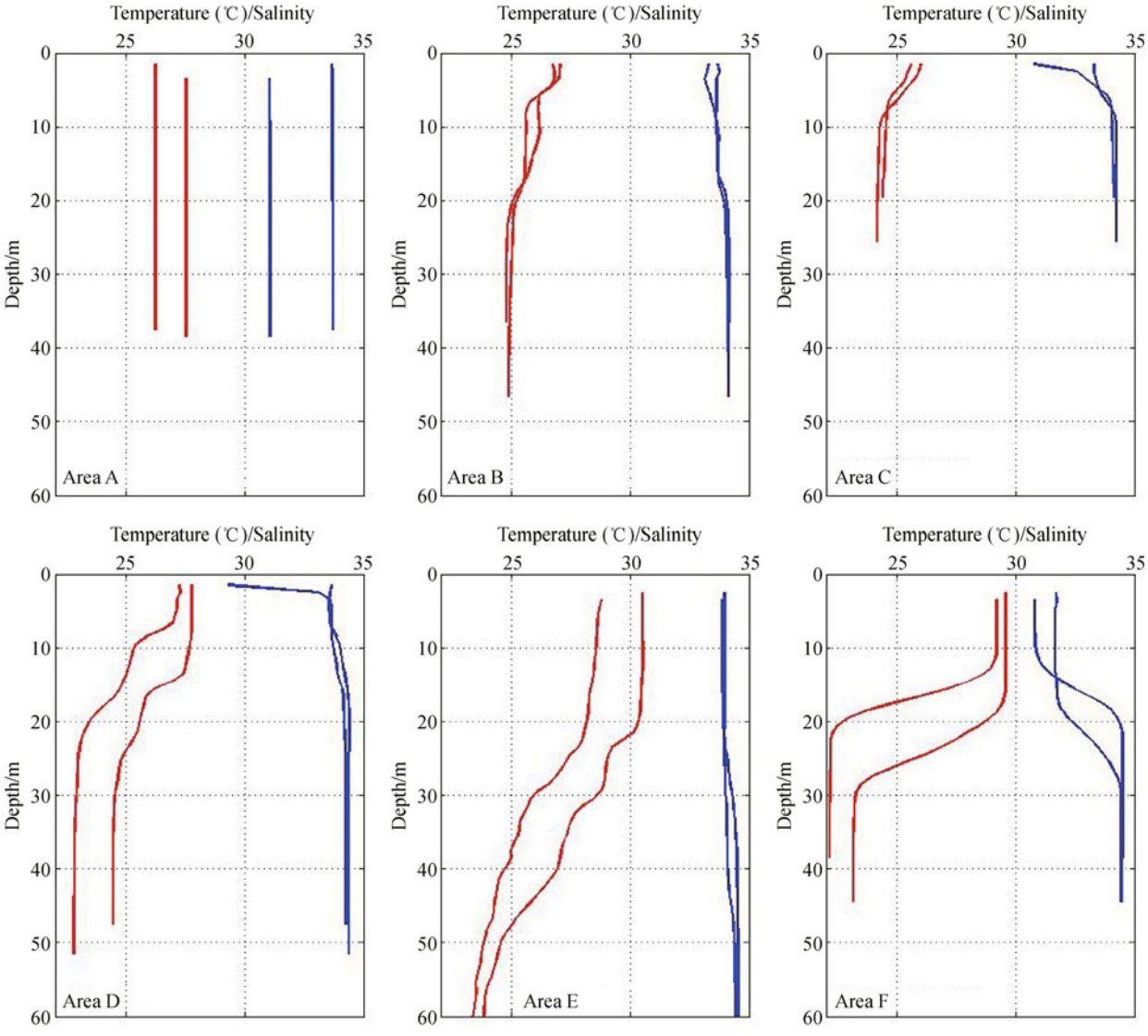

Fig. 4 Typical profiles of temperature (red) and salinity (blue) in Areas A–F.

in Area E is 0.48, similar to that in Areas B and C. Note that in Area F, the water is highly stratified (see Fig. 4) due to the intrusion of the diluted water originating from the Pearl River (Hong et al., 2009). The vertical gradients of temperature and salinity in the thermocline (halocline) reach 1.00°C·m^{-1} and 0.58 m^{-1}, respectively. It is evident from Fig. 3(b) and the spatial distribution of surface salinity (not shown) that the diluted water enters into the TWS along the west edge of the TB.

The Simpson-Hunter parameter K calculated from the modeled tidal currents is shown in Fig. 5. By visual inspection, one can easily identify that the spatial distribution of K seems to suggest similar features to the STDs of temperature and salinity shown in Fig. 3. For example, in Area A, the K value is mostly below 2.0, suggesting very strong tidal mixing, consistent with the well-mixed structure of temperature and salinity and supported by direct measurements of the turbulent kinetic energy dissipation rate ε of 10^{-7}–10^{-5} W·kg^{-1} (Fig. 6). Note that the dissipation rate is ~10^{-10} W·kg^{-1} in the deep ocean (Thorpe, 2004) and about 10^{-7}–10^{-5} W·kg^{-1} in tidally energetic shelf waters (Liu et al., 2009). Tidal mixing is weakest, with K above 3.0, in the cross-strait band from Meizhou (MZ) to Wuci (WC) and it is moderate in the middle TWS, with K of 2.0–2.8.

To quantify the correlations between tidal mixing and the STDs of temperature and salinity, we calculate the mean value of K as well as STDs in each of the six areas (A–F). The results are shown in Fig. 7. One can see that the STD_1 and K are highly correlated, with a correlation coefficient as high as 0.994, suggesting the dominant role of tidal mixing in setting up thermal structures in the TWS. A linear regression of the K versus STD_1 relationship gives a value (K_c) of 1.78 for the critical Simpson-Hunter

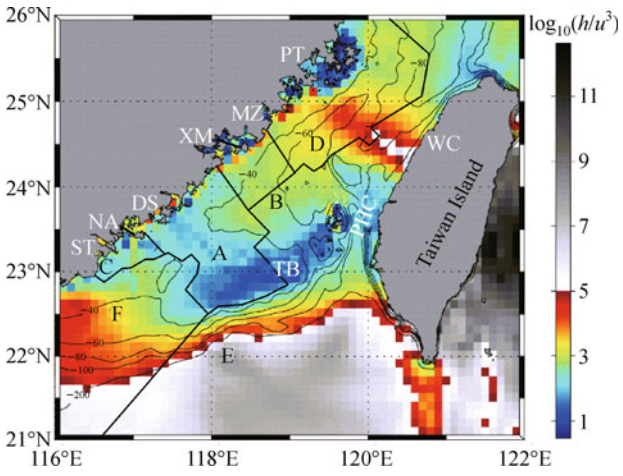

Fig. 5 Distribution of tidal mixing parameter (K). The areas where $K < 5$ are filled with color, and the area with $K > 5$ are filled in gray. Acronyms: PT-Pingtan, MZ-Meizhou, XM-Xiamen, DS-Dongshan, NA-Nanao, ST-Shantou, WC-Wuci, TB-Taiwan Bank, PH-Penghu Archipelago, PHC-Penghu Channel.

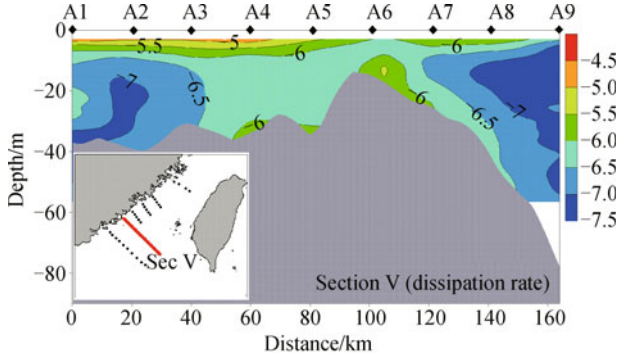

Fig. 6 Distribution of the turbulent kinetic energy dissipation rate ($\log_{10}[\varepsilon\ (\mathrm{W \cdot kg^{-1}})]$) along section V. The section location is shown in the lower left inset.

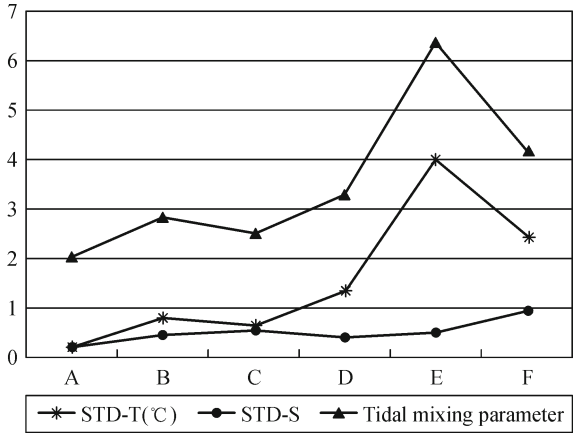

Fig. 7 Comparison of STDs of temperature (T) and salinity (S), and tidal mixing parameter K in Areas A–F.

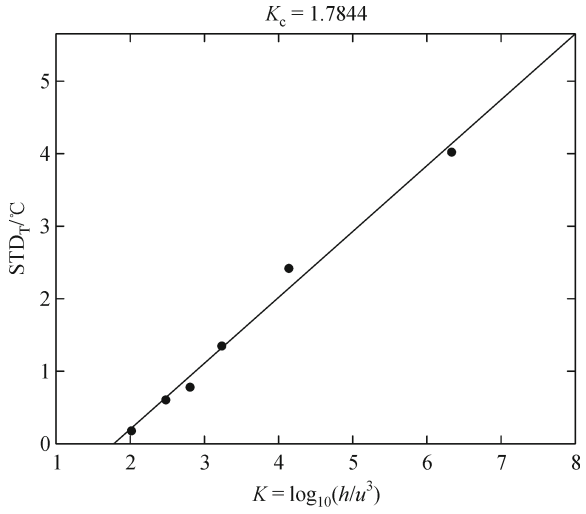

Fig. 8 Linear regression of the K versus $\mathrm{STD_1}$ relationship.

parameter of this region (Fig. 8). In contrast, the correlation between K and $\mathrm{STD_2}$ is much weaker. This is because the variation of salinity is not dependent on the solar radiation, which is relatively uniform within a coastal region, but is greatly affected by the localized freshwater and/or salt fluxes. In the present case, as shown later, the spatial distribution of salinity in the TWS is under significant influence of tidal mixing and river plumes.

The above analysis indicates that tidal mixing is the main cause of the variations of thermohaline structure in the TWS. Therefore, we suggest define the critical tidal mixing parameter $K_c = 1.78$ as a threshold value for classifying stratified and mixed areas in the TWS.

3.2 Fronts in the TWS: a tale of three processes

The analysis in Sect. 3.1 indicates that the thermohaline structure in the TWS is essentially determined by the spatial variation of tidal mixing. However, a close look at the spatial distributions of temperature and salinity reveals that in some regions of the strait upwelling and river plumes may also play important roles. For example, in situ measurements and satellite observations have revealed the existence of three distinct upwelling-induced cold zones in the TWS (Hu et al., 2003a; Lan et al., 2009), located in the offshore areas of Dongshan, Pingtan and at the outer edge of the TB. As shown in Fig. 9(a), the SST in these cold zones is typically 2–3°C lower than that in the surrounding waters.

The upwelling nature of these zones is evident in the cross-isobath sections of temperature and salinity (Fig. 10). The shoreward uplift of isothermals and isohalines along transects I, II, V, and VI shows that upwelling is predominant in the offshore areas of Pingtan, Meizhou, Dongshan and Nanao. The dome structures of temperature and salinity along transects III and IV are results of the

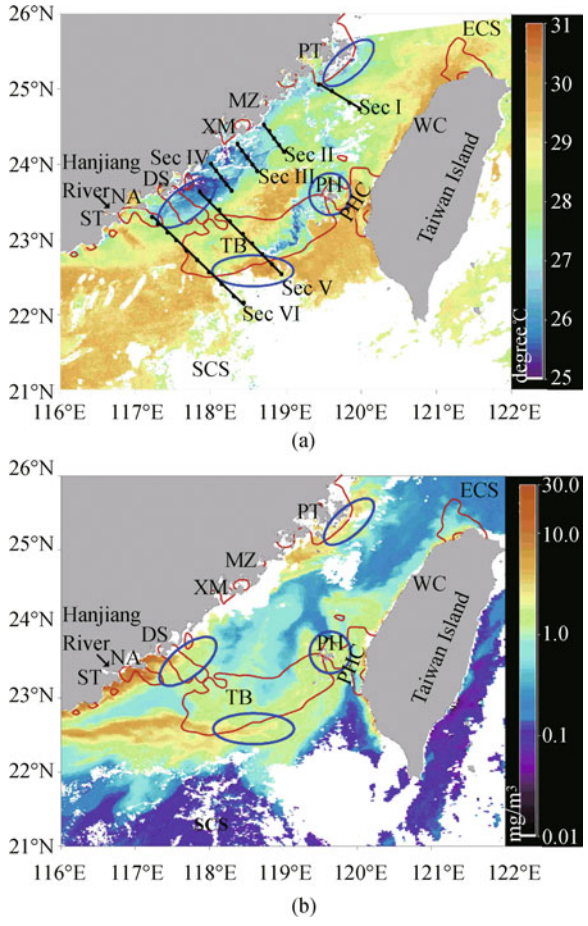

Fig. 9 MODIS images of (a) SST on August 20, 2008 and (b) Chl-*a* on July 9, 2009. The contours for the critical tidal mixing parameter (K_c = 1.78) are shown in red. Sections I–VI are shown with black lines. Locations of the summertime upwelling cores in the TWS are shown with blue ellipses (adapted from Hu et al. (2003a)). Acronyms: PT-Pingtan, MZ-Meizhou, XM-Xiamen, DS-Dongshan, NA-Nanao, ST-Shantou, WC-Wuci, TB-Taiwan Bank, PH-Penghu Archipelago, PHC-Penghu Channel, SCS-South China Sea, ECS-East China Sea.

upwelling at their middle part. Similarly, the dome structure of temperature and salinity between Sts. A7 and A8 in transect V is due to upwelling at the outer edge of TB. As a result, the fronts of temperature and salinity are formed on both sides of the upwelling band. The horizontal gradients of temperature and salinity reach 0.2°C·km^{-1} and 0.05 km^{-1}. A well-mixed high temperature low salinity water at Sts. A3–A6 is sandwiched between two upwelled waters in transect V. The temperature is above 26°C and the salinity is below 33.20.

The upwelling influences in the TWS can be further illustrated by the spatial distribution of Chl-*a* concentration, and the influence of river plumes is most striking in satellite images (Fig. 9(b)). One can see that there are three distinct high Chl-*a* concentration zones in Fig. 9(b): one located near the Pingtan Island, one in the offshore area of Nanao, and a zonal band along 22.5°N extending from the coast to about 119°E. Fronts of Chl-*a* concentration naturally formed at the edges of the high concentration zones. Comparing Figs. 9(a) and 9(b) one can figure out that the high Chl-*a* concentration zone near the Pingtan Island is a result of upwelling, while the other two high Chl-*a* concentration zones are signatures of river plumes originating from the Hanjiang River and the Pearl River (Li et al., 1998; Zhuang et al., 2003; Hong et al., 2009). The plume structure is also evident in the salinity sections of V and VI as shown in Fig. 10. The surface salinity is below 32.60 at Sts. A3–A7 and B4–B7, showing a definite feature of diluted waters.

To illustrate the joint control of tidal mixing, river plumes and upwelling in setting up thermohaline structures and nutrient loading in the TWS, the contours of critical Simpson-Hunter parameter K_c = 1.78 are overlaid in Fig. 9. One can see that the SST and Chl-*a* fronts do not coincide well with them. This means that the fronts of SST and Chl-*a* in the TWS are not only simply determined by tidal mixing, but also under significant influences of upwelling and river plumes. Therefore, thermohaline fronts and Chl-*a* fronts in the TWS cannot simply be predicted by the Simpson-Hunter parameter, even though the spatial variations of stratification (characterized by STD_1) are essentially determined by tidal mixing as shown in Sect. 3.1. One needs to consider all the three major processes when evaluating spatial variations of thermohaline and biogeochemical parameters in the TWS.

4 Discussion

It is interesting to note the "sandwich" structure in midsection V (Fig. 10), an entire well-mixed water mass with temperature above 26°C and salinity below 33.2 at Sts. A3–A6 located between the upwelling waters with low temperature on both sides. Correspondingly, in Fig. 6, a high dissipation rate ~ 10^{-6} W·kg^{-1} appears at Sts. A3–A7 and the dissipation rate ~ 10^{-7} W·kg^{-1} appears on both sides (near shore and at Sts. A7–A9). The Sts. A3~A7 are just located in the TB strong tidal mixing area (within the contour lines K = 1.78 shown in Fig. 9(a)). Therefore, we suppose that the structure of the water on the TB (Sts. A3–A7) is mainly dominated by strong tidal mixing, while the thermohaline structure at Sts. A7–A9 is mainly controlled by TB upwelling. Moreover, the dissipation rate ~ 3×10^{-7} W·kg^{-1} can be taken as a dynamic balance boundary between the strong tidal mixing and upwelling. Therefore, we consider that the "sandwich" structure of temperature and salinity can be attributed to the balance of the tidal mixing and upwelling. We further suppose that the strong tidal mixing at the TB mixes the high salinity water from upwelling with the diluted water from the Pearl River, and the strong tidal mixing weakens the characteristics of the upwelling and diluted water at the same time.

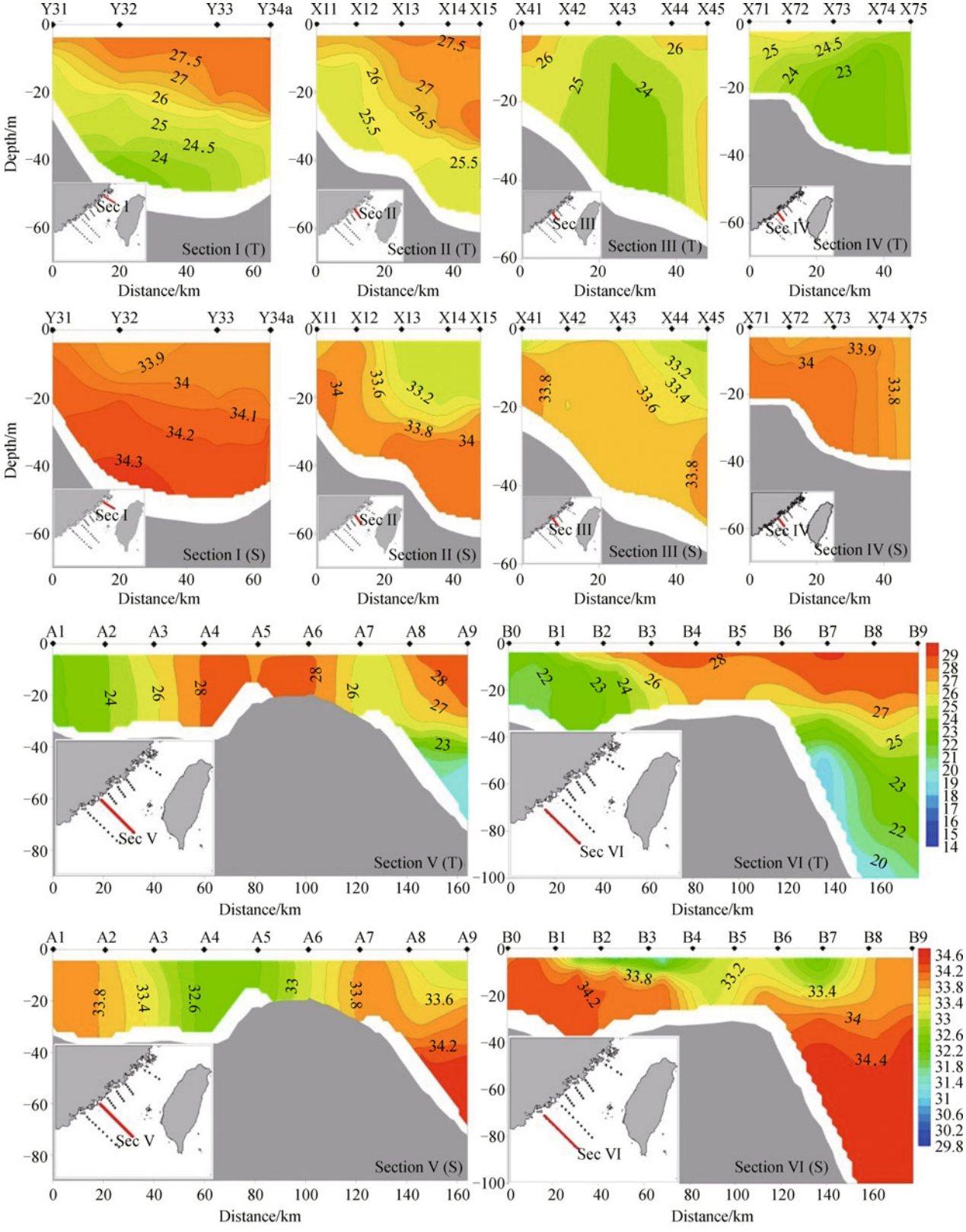

Fig. 10 Sectional distributions of temperature (°C) and salinity at sections I–VI. The section locations are shown in the lower left insets.

5 Summary

In this paper, based on eight years of in situ hydrographic observations, satellite images of SST, and Chl-*a* concentration, and results of a two-dimensional tidal model, we investigate summer stratification in the TWS and its dependence on tidal mixing in the context of Simpson and Hunter's (1974) energetic arguments, as well as upwelling and river plumes. The major results are as follows.

As in other tidally energetic shelf waters, thermohaline structure in the TWS is to the first order determined by the spatial variation of tidal mixing. The stratification characterized by STD_1 is highly correlated with the Simpson-Hunter parameter.

The tidally well-mixed regions are mainly located on the TB and offshore waters off the Dongshan Island, Nanao Island and Pingtan Island, while the northern and central TWS and the region south of the TB are stratified. The critical Simpson-Hunter parameter in the regions is estimated to be 1.78.

An accurate evaluation of the thermohaline structure and spatial distribution of biogeochemical parameters (e.g., Chl-*a*) in the TWS needs to consider the influences of upwelling and river plumes. In the other words, the fronts in the TWS are results of joint control of tidal mixing, upwelling, and river plumes.

Acknowledgements This research was jointly supported by the National Basic Research Program of China (No. 2009CB21208) and the National Natural Science Foundation of China (Grant Nos. 41121091, 41006017, 40810069004 and 40576015).

References

Chang Y, Shimada T, Lee M A, Lu H J, Sakaida F, Kawamura H (2006). Wintertime sea surface temperature fronts in the Taiwan Strait. Geophys Res Lett, 33(23): L23603

Chuang W S (1986). A note on the driving mechanism of the current in the Taiwan Strait. J Oceanogr Soc, 42(5): 355–361

Dietrich G (1951). Influences of tidal streams on oceanographic and climatic conditions in the sea as exemplified by the English Chanel. Nature, 168(4262): 8–11

Gan J, Li L, Wang D X, Guo X G (2009). Interaction of a river plume with coastal upwelling in the northeastern South China Sea. Cont Shelf Res, 29(4): 728–740

Garrett C, Maas L (1993). Tides and their effects. Oceanus, 36: 27–37

Holt J, Umlauf L (2008). Modeling the tidal mixing fronts and seasonal stratification of the Northwest European Continental shelf. Cont Shelf Res, 28(7): 887–903

Hong H S, Zheng Q A, Hu J Y, Chen Z Z, Li C Y, Jiang Y W, Wan Z W (2009). Three-dimensional structure of a low salinity tongue in the southern Taiwan Strait observed in the summer of 2005. Acta Oceanol Sin, 28(4): 1–7

Hu J Y, Kawamura H, Hong H S, Pan W R (2003a). A review of research on the upwelling in the Taiwan Strait. Bull Mar Sci, 73(3): 605–628

Hu J Y, Kawamura H, Hong H S, Suetsugu M, Lin M S (2001). Hydrographic and satellite observations of summertime upwelling in the Taiwan Strait: a preliminary description. Terr Atmos Ocean Sci, 12: 415–430

Hu J Y, Kawamura H, Tang D L (2003b). Tidal front around the Hainan Island, northwest of the South China Sea. J Geophys Res (Oceans), 108: 1–9

Jan S, Wang J, Chern C S, Chao S Y (2002). Seasonal variation of the circulation in the Taiwan Strait. J Mar Syst, 35(3–4): 249–268

Jan S, Wang Y H, Chao S Y, Wang D P (2001). Development of a Nowcast System for the Taiwan Strait (TSNOW): numerical simulation of barotropic tides. Ocean Polar Res, 23(2): 195–203

Lan K W, Kawamura H, Lee M A, Chang Y, Chan J W, Liao C H (2009). Summertime sea surface temperature fronts associated with upwelling around the Taiwan Bank. Cont Shelf Res, 29(7): 903–910

Li L, Guo X, Wu R (2000). Oceanic fronts in southern Taiwan Strait. J Oceanogr Taiwan, 19: 147–156

Li L, Jr Nowlin W, Su J L (1998). Anticyclonic rings from Kuroshio in the South China Sea. Deep-Sea Res, 45(9I): 1469–1482

Liu Z Y, Wei H, Lozovatsky I D, Fernando H J S (2009). Late summer stratification, internal waves, and turbulence in the Yellow Sea. J Mar Syst, 77(4): 459–472

Lü X G, Qiao F L, Xia C S, Yuan Y L (2007). Tidally induced upwelling off Yangtze River estuary and in Zhejiang coastal waters in summer. Sci China Ser D-Earth Sci, 50(3): 462–473

Qiu Z F, Hu J Y, Chen Z Z (2002). Harmonic analysis on multi-day series current data at two anchored stations in the south Taiwan Strait. Mark Sci, 26(7): 50–53 (in Chinese with English abstract)

Shang S L, Zhang C Y, Hong H S, Shang S P, Chai F (2004). Short-term variability of chlorophyll associated with upwelling events in the Taiwan Strait during the southwest monsoon of 1998. Deep sea Res. II: Topical studies in Oceanography, 51: 1113–1127

Simpson J H, Hunter J R (1974). Fronts in the Irish Sea. Nature, 250 (5465): 404–406

Tang D L, Kester D R, Ni I H, Kawamura H, Hong H S (2002). Upwelling in the Taiwan Strait during the summer monsoon detected by satellite and shipboard measurements. Remote Sens Environ, 83 (3): 457–471

Thorpe S A (2004). Recent developments in the study of ocean turbulence. Annu Rev Earth Planet Sci, 32(1): 91–109

Zhao B R (1985). The fronts of the Huanghai Sea cold water mass induced by tidal mixing. Oceanol Limnol Sin, 16(6): 451–460 (in Chinese with English abstract)

Zhu J, Hu J Y, Zhang W Z, Zeng G N, Chen D W, Chen J Q, Shang S P (2009). Numerical study on Tides in the Taiwan Strait and its adjacent areas. Marine Science Bulletin, 11(2): 23–36

Zhuang W, Hu J Y, He Z G, Zeng G N, Chen Z Z (2003). An analysis on surface temperature and salinity from southern Taiwan Strait to Zhujiang River Estuary during July–August, 2000. J Tropical Oceanog, 22: 68–76 (in Chinese with English abstract)

AUTHOR BIOGRAPHIES

Ms. Jia Zhu obtained her B.S. (2003) and M.S. (2006) degrees in

physical oceanography from Xiamen University. She is currently an engineer in State Key Laboratory of Marine Environmental Science (Xiamen University). Her fields of research include hydrodynamic process analysis based on the marine field observations, water mass analysis and numerical study on tides. E-mail: zhujia@xmu.edu.cn

Dr. Jianyu Hu obtained his Ph.D degree (2001) in physical oceanography from Tohoku University of Japan and Ph.D degree (2002) in environmental science from Xiamen University of China. He is now a professor in State Key Laboratory of Marine Environmental Science and Department of Physical Oceanography at Xiamen University, focusing on the study of regional environmental oceanography. E-mail: hujy@xmu.edu.cn

Dr. Zhiyu Liu obtained his B.S. (2004) and Ph.D (2009) degrees in physical oceanography from Ocean University of China. During his Ph.D. study he spent 18 months in the School of Ocean Sciences at Bangor University, UK, working with Prof. Steve Thorpe FRS on the instability of stratified shear flows. He joined the State Key Laboratory of Marine Environmental Science and Department of Physical Oceanography at Xiamen University in 2009, where he is currently holding an associate professorship. His area of expertise includes internal waves, turbulence and mixing in the ocean, stability of stratified shear flows, physical oceanography of coastal and shelf seas, upper ocean dynamics, and geophysical fluid dynamics. E-mail: zyliu@xmu.edu.cn